Geochimica et Cosmochimica Acta Vol. 56, pp. 1507–1521

0016-7037/92/$5.00 + .00

Effect of iron diagenesis on the transport of colloidal clay in an unconfined sand aquifer

JOSEPH N. RYAN and PHILIP M. GSCHWEND

Water Resources and Environmental Engineering, Department of Civil Engineering, Massachusetts Institute of Technology, Cambridge, Massachusetts 02139, USA

(*Received July* 12, 1991; *accepted in revised form January* 15, 1992)

Abstract—The role of Fe diagenesis in the transport of clay colloids was investigated in the Cohansey Sand, an Fe(III) oxide-coated quartz arenite that covers most of the New Jersey Coastal Plain. Based on our past work, we hypothesized that clay had been transported into the sediments, that the clay distribution was controlled by attachment to surface Fe(III) oxides, and that anoxic water infiltrating from a swamp had dissolved Fe(III) oxides and released clay colloids into flowing groundwater. Sediment cores were collected from upland and swamp terrains, and the composition and distribution of the clay-sized and heavy mineral fractions were examined by X-ray diffraction, optical and electron microscopy, separations, and elemental analyses. Throughout the upland core and below 6.1 m in the swamp core, oxidized soil and sediment layers contained goethite and >15 μmol g^{-1} surface Fe (extractable by Ti(III) reduction), but the swamp-reduced soils and sediments lacked goethite and contained <5 μmol g^{-1} surface Fe. The clay-sized content of the oxidized sediments was roughly double that of the reduced sediments. Electron microscopy revealed that coatings on the quartz grains had the appearance of infiltrated clay particles. The relationship between clay and surface Fe content indicated that the onset of reducing conditions below the swamp remobilized clay colloids by dissolving Fe(III) oxide cement. Surface Fe(III) oxides were derived from weathering of ilmenite and pseudorutile, Fe-Ti oxides found in the heavy mineral fraction. In the oxidized sediments, Fe was transported from the Fe-Ti oxide grains to quartz surfaces, where it was deposited as surface Fe(III) oxides mixed with kaolinite. Thus, the weathering of Fe-bearing minerals and the formation and dissolution of secondary Fe(III) oxides influenced the mobility of colloidal clay in the Cohansey Sand.

INTRODUCTION

THE TRANSPORT OF RADIONUCLIDES, metals, and hydrophobic organic compounds through aquifers and laboratory soil columns is enhanced by sorption to mobile colloidal phases (GIBLIN et al., 1981; BROWNAWELL and FARRINGTON, 1986; SHORT et al., 1988; BUDDEMEIER and HUNT, 1988; ENFIELD and BENGTSSON, 1988; PENROSE et al., 1990; MAGARITZ et al., 1990). Colloidal material may also be implicated in the mobilization of ore metals (HORZEMPA and HELZ, 1979; TURNER-PETERSON, 1985). The degree of enhancement or mobilization depends on the abundance and nature of colloids present, the extent of association with colloids, and the transport of colloids through the porous medium. While the sorption of low-solubility species to colloidal phases and the transport of colloids through porous media have been investigated and even quantitatively modeled with some success, only a few researchers have studied the factors that influence the abundance and nature of colloids in groundwater (e.g., LANGMUIR, 1969; KHILAR and FOGLER, 1984; DEGUELDRE et al., 1989). With this in mind, we undertook a study of the geochemical conditions that produced widely varying concentrations of suspended clay particles in a sandy surficial aquifer located on the Atlantic Coastal Plain.

Unconfined sandy aquifers composed primarily of Fe(III) oxide-coated quartz are common on the Atlantic Coastal Plain. In past work, we investigated groundwater from a surficial aquifer on the New Jersey Coastal Plain, the Cohansey Sand (RYAN and GSCHWEND, 1990). The groundwater was collected from two wells located only 60 m apart, one screened 8 m below the peat layer of a swamp ("swamp") and the other screened 10 m below highly permeable soils in the nearby uplands ("upland"). The groundwater below the swamp contained ≤30 μM dissolved oxygen and 60 mg L^{-1} colloids, mainly kaolinite fragments; but colloids were absent from the oxic groundwater below the upland terrain. We hypothesized that clay colloids were removed from suspension by Fe(III) oxide coatings on the quartz grains in the oxic zone of the aquifer. In contrast, clay transport was facilitated below the swamp because Fe(III) oxide coatings were absent in the anoxic zone.

To test the hypothesis that clay transport was controlled by the presence of Fe(III) oxide coatings, we collected soil and sediment cores near the groundwater wells to examine distributions of minerals and elements and grain-scale mineral associations. We assumed that clay abundance in the porewater would be inversely related to the clay content of the soil and sediment; therefore, variations in the abundance of the clay-sized fraction and surface Fe in the oxidized and reduced soil and sediment layers were examined. We also wanted to determine the role of Fe diagenesis in clay transport, so we investigated the appearance and composition of the Fe-bearing primary minerals and secondary Fe(III) oxides.

METHODS AND MATERIALS

Site Description

Two core samples were collected near the head of the McDonalds Branch watershed in Lebanon State Forest, southern New Jersey in August 1989 (Fig. 1). The site is located in a low-relief, pine-dominated region of the New Jersey Coastal Plain known as the Pine Barrens. The cores were taken from two locations (upland and swamp) about 50 m down-gradient from groundwater wells sampled

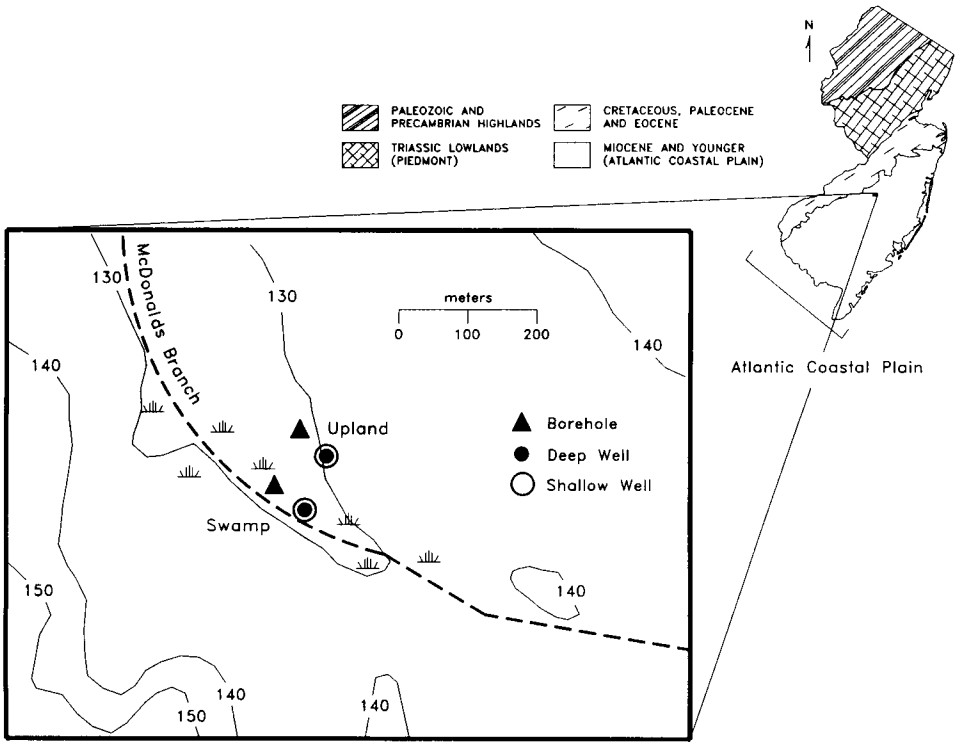

FIG. 1. Sampling site showing location of sampling site in relation to the geological provinces of New Jersey (after OLSSON, 1963), topography (contours in feet), intermittent stream (McDonalds Branch), boreholes, and wells sampled previously (RYAN and GSCHWEND, 1990).

in the previous study (RYAN and GSCHWEND, 1990) to prevent contamination of the wells.

The surficial aquifer underlying of most of the Pine Barrens is the Late Miocene Cohansey Sand, a poorly sorted quartz arenite wedge, 0–61 m thick, composed of marine sheet sands intercalated with distributary, swamp, and marsh deposits (CARTER, 1978). Laminated clays deposited in tidal channels and marshes are usually thin (<1 m) but laterally extensive, spanning distances of hundreds of meters (RHODEHAMEL, 1979a). Overall, however, clay is a minor constituent of the Cohansey (generally less than 5–10%). Moderate wave energy separated the sediment load by size and density, leaving sand layers relatively clay-free (CARTER, 1978). The sand fraction in the Cohansey is made up almost entirely of quartz, usually coated by goethite, ≤3% heavy mineral grains (85% ilmenite and its weathering products; MARKEWITZ, 1969), and trace amounts of feldspar and muscovite. The clay and silt fractions are dominated by kaolinite, with trace amounts of muscovite, illite, and quartz (RHODEHAMEL, 1979a).

Deposition of the Cohansey Sand began about 20 million years ago and ended about 5 million years ago when the sea completed its final regression from the New Jersey Coastal Plain (RHODEHAMEL, 1979a). During the Pleistocene, glaciers lowered sea levels more than 100 m below the present level, resulting in vigorous and continuous fluvial and aeolian erosion and redeposition of Cohansey sediments. During the most recent glaciation (Wisconsin, 100,000 to 10,000 years ago), the Pine Barrens may have resembled present-day northern Greenland, with strong winds blowing off ice sheets over a sandy surface devoid of vegetation (MINARD, 1966). Following the Wisconsin, the topography and flora of the region took on its present form. Ecologically, the Pine Barrens can be divided into two distinct systems: (1) uplands, characterized by pine-oak vegetation and well-drained soils; and (2) lowlands, distinguished by cedar and hardwood swamps, *Sphagnum*, and soils made up of muck and peat (LITTLE, 1979).

The groundwater hydrology of the site may be influenced by the strike and dip of a thick (<1 m) impermeable clay-silt layer below the permeable sands of the unconfined aquifer (LORD et al., 1990). Local groundwater flow directions and gradients were estimated from hydraulic head measurements in the four groundwater wells (Fig. 1). Downward hydraulic gradients appear to exist between the shallow and deep swamp wells (0.17 $m \cdot m^{-1}$) and between the shallow swamp and deep upland wells (0.02 $m \cdot m^{-1}$) but not between the shallow and deep upland wells. The hydraulic head data suggest that the swampy area around McDonalds Branch is a recharge zone (assuming that groundwater sampled by these wells is hydraulically connected) despite its location in a topographic depression.

Field Procedures

The boreholes were drilled without fluids using hollow-stem augers at locations geographically similar to the locations of the groundwater wells upstream (Fig. 1). The core samples were collected using a 61 cm steel split-tube sampler lined with 3.8 cm inside-diameter clear cellulose acetate butyrate (CAB) tubes. Plastic basket retainers were used to hold the unconsolidated samples in the sampler during withdrawal. The split-tube sampler was driven into the sediment with a 63.5 kg hammer, and the CAB tube with the sediments was removed, capped, and stored upright in a cooler. The sampler was washed and rinsed with distilled water between samples.

The sampler was driven into the undisturbed sediment below the auger. Two samples were taken for every 1.5 m section of auger added to the drill string until we reached wet, unconsolidated sand that entered the auger flight and inhibited sampling of undisturbed sediment. At these points, we measured the distance that running sands penetrated the auger to determine how much of each sample was collected outside the auger. The split-tube sampler retrieved undisturbed samples representing about 71% of the upland soil and sediment above 5.8 m and about 53% of the swamp soil and sediment. Below 5.8 m in the upland core, running sands became so fluid that samples could not be taken below the auger because the auger was filled to heights greater than the length of the split-tube sampler. Consequently, samples from below 5.8 m were retrieved from the

auger flights and placed in plastic zipper-lock bags. We stopped drilling when we reached the thick clay-silt layer at depths of about 10 m below the uplands and 8 m below the swamp.

Laboratory Procedures

The cores were split and subsampled (based on changes in sediment color and texture) for chemical analyses and preparation of oriented thin sections. Subsamples were collected from core centers to avoid edge smearing and contamination.

Total Fe, Al, and Ti for the sediments were determined by HF/HCl/HNO_3 digestion of 0.1 g portions of the samples in Teflon™-lined bombs at 110°C for 1 h (LIM and JACKSON, 1982) and inductively coupled plasma/atomic emission spectroscopy (ICP/AES). Calibration curves were prepared with blanks and standards made up with the digestion solution. Method precision for triplicate analyses of two samples was [Fe] ± 8%, [Ti] ± 5%, and [Al] ± 14%.

"Surface" Fe and Al were determined by selective dissolution of the Fe(III) oxide fraction using the Ti(III)-citrate-ethylenediaminetetraacetate (EDTA) ternary complex as the reductant (RYAN and GSCHWEND, 1991). The reducing solution was combined with sample portions (0.3 g), sonicated for 5 min, shaken for 10 min, and centrifuged at 26,900 g (maximum) for 1 h. The supernatant was analyzed for Fe and Al by ICP/AES. The extractions were repeated until the amount of Fe removed in the last extraction was <5% of the cumulative removed. In almost all of the samples, Fe was >95% removed in the first extraction; however, in three of the samples from the swamp-reduced sediments, more than two extractions were required. The method precision for quintuplicate analyses of three samples was [Fe] ± 3% and [Al] ± 6%. Fe and Al removed by this method are presumed to include organically bound elements and amorphous and crystalline oxides. Fe and Al left behind are referred to as "structural" Fe and Al and are presumed to reside in aluminosilicates and Fe(II)-bearing oxides.

Organic matter content was determined gravimetrically by loss on ignition. Sample portions (5–10 g) were dried at 105°C for 6 h and combusted at 450°C for 6 h and desiccated prior to weighing. Method precision for duplicate analyses of six samples was ±12%.

Clay-sized (<2 μm) content was determined by sonication and sedimentation of suspensions of 0.5 g sample portions in 30 mL distilled water. The suspension was sonicated for 10 min in an 80 W sonicating bath and added to a cylinder containing 1 L distilled water. Sonication appeared to adequately dislodge clay- and silt-sized minerals from the sand-sized grains. The turbidity of the <2 μm suspensions were compared to a turbidity calibration curve made using dilutions of a 500 mg L^{-1} < 2 μm "colloidal kaolin powder" (EM Science, Cherry Hill, NJ) stock solution separated by the same method. Method precision for six duplicate samples was ±12%.

Heavy mineral content was determined by suspending 5–10 g portions of selected samples in 100 mL of bromoform ($CHBr_3$; specific gravity 2.89) in a separatory funnel. The suspensions were shaken and allowed to settle for 5 min two times, then the heavy minerals were trapped on filter paper. The entire procedure was repeated for the heavy minerals trapped in the first separation. Method precision for four duplicate samples was ±8%.

Minerals of whole sediments, clay-sized fractions, and heavy mineral fractions were identified by powder X-ray diffraction (XRD) using a Diano XRD-5 diffractometer with Ni-filtered Cu Kα radiation (35 kV, 15 mA, 3° divergence slit, 1° scatter slit, and 0.2 mm receiving slit, 2° 2θ min^{-1} scan rate). Randomly oriented mounts of whole sediment samples were prepared by drying in a desiccator, grinding by mortar and pestle to pass through a 400-mesh (<37 μm) sieve, and packing into Al sample holders. Oriented samples of the <2 μm clay suspensions were prepared by vacuum-filtering the suspensions through Nuclepore 0.45 μm Ag membrane filters (POPPE and HATHAWAY, 1979). Identification of clay mineral peaks was aided by glycolation and heating. The heavy minerals were ground to pass through a 400-mesh sieve, suspended in distilled water, and vacuum-filtered onto Ag membrane filters. The raw diffraction patterns were digitized, and the 2θ angles were calibrated to the sharp Ag peak at d = 2.044 Å.

Thin sections of oriented samples were prepared by Mineral Optics, Inc. (Wilder, VT) by vacuum-impregnating with epoxy and diamond-polishing selected subsamples. Modal abundances of grain types and pore fillings were determined by 400-point counts per sample. Quartz grain sizes were also determined for 100 grains in each sample. The thin sections were also examined by environmental scanning electron microscopy (ESEM; ElectroScan Inc., Wilmington, MA) at 20–30 kV accelerating voltage. Uncoated thin sections were attached to stubs with carbon tape and placed in a sample chamber under a water vapor atmosphere of 2–10 Torr.

Selected whole sediment, thin section, and heavy mineral samples were examined by SEM and energy-dispersive X-ray (EDX) spectroscopy with a Cambridge Stereoscan 240 SEM and Link EDX. The heavy mineral samples were suspended in distilled water and sonicated for 10 min to remove particles obscuring surface features. Samples were air-dried, Au-coated, and analyzed in backscatter and secondary electron mode at accelerating voltages of 20 and 30 kV. Element profiles across quartz grain coatings were acquired in some samples by a series of spot EDX analyses made at intervals in a path across the coating perpendicular to the quartz surfaces. Spot surface and wide-area interior EDX analyses were made in Fe-Ti oxide grains. EDX spectra were acquired at rates of 1000–3000 counts s^{-1} in 100 s scans and converted to molar concentrations of Fe, Al, Si, Ti, K, Cl (epoxy), and Au (coating) using built-in X-ray absorption, fluorescence, and atomic number corrections.

RESULTS

Soil and Sediment Description

The upland and swamp cores both exhibited well-developed soil zones containing organic detritus, thick sandy layers, and thin (≤3 cm), dark, fine-grained layers from the surface to depths of 2.3 m. The sandy layers of the upland soils appeared light gray to very pale brown (dry sediments, 10YR7/1 to 10YR7/3, Munsell Soil Color Chart). The swamp soils appeared gray to light brownish gray (10YR6/1 to 10YR6/2). The water table approximately coincided with the bottom of the soil zone in the upland core and was at the surface in the swamp. Below the soil zone (>2.3 m depth), upland sediments consisted of unconsolidated very pale brown to yellow (10YR7/3 to 10YR7/8) sands. The swamp sediments also consisted mainly of unconsolidated sands. Swamp sediment color changed distinctly at 6.1 m from white to light gray (5YR8/1 to 5YR7/1) above to yellow to reddish yellow (10YR8/6 to 7.5YR6/6) below. The color boundary did not coincide with any abrupt change in sediment grain size.

Thin-section point counting showed that the sediments consisted mainly of subrounded quartz grains (Table 1). Other grains identified in minor and trace quantities included opaque and transparent heavy minerals (identified as zircon and augite), feldspar, and mica. The fine-grained matrix fillings and coatings were evenly dispersed throughout the sediments and showed no preferred orientation. They often extended into and blocked the smaller pore spaces between grains. Sediments from the upland core and those from below 6.1 m in the swamp core contained slightly more matrix and coating than the swamp sediments and soils above 6.1 m (13.8 ± 3.8% vs. 9.0 ± 5.2%). Greater than 90% of the quartz grains were between 0.25 and 1.0 mm in diameter. The quartz grain size distributions of the samples were quite similar; thus, we interpreted changes in clay and surface Fe content as the result of post-depositional processes.

The white to light gray color of the swamp soil and sediments above 6.1 m suggested an apparent lack of Fe(III) oxides, so we assumed that water infiltrating through the peat layer below the swamp was rich in organic matter, anoxic,

Table 1. Results of thin section point counting for selected samples. Headings include quarts (qts), feldspar and mica (fsp + mica), heavy minerals (hvy min), matrix and coatings (matx + coat) and void space (void).

sample	depth (m)	qts (%)	fsp+ mica (%)	hvy min (%)	matx+ coat (%)	void (%)
Upland						
U.2.2	0.8–1.5	56.5	0.5	2.2	14.0	26.8
U.3.2	1.7–2.0	57.5	0.8	1.5	16.2	24.0
U.4.3	2.4–2.8	53.5	0.5	1.0	17.0	28.0
U.6.1	3.7–4.1	59.2	0.5	0.5	6.0	33.8
U.8.1*	4.9–5.3	52.8	0.5	0.8	13.0	33.0
Swamp						
S.1.3	0.6–0.9	65.5	0.8	1.5	5.2	27.2
S.3.3	1.6–1.8	57.0	0.8	1.2	19.2	21.8
S.4.1	2.3–2.4	60.2	0.5	0.8	10.5	28.0
S.5.1	2.7–3.3	59.2	0.2	1.2	9.8	29.5
S.7.1	4.3–4.6	52.5	0.5	1.2	6.2	39.5
S.8.1	5.8–6.1	61.5	0.2	2.2	3.2	32.8
S.8.2	6.1–6.3	61.0	0.0	0.2	16.8	22.0

*Sample U.8.1 is not an oriented sample.

and acidic, like the swamp groundwater sampled 50 m upstream (RYAN and GSCHWEND, 1990). The pale brown to yellow color of the upland soil and sediment and the swamp sediment below 6.1 m suggested that this groundwater was oxic and that Fe(III) oxide formation was promoted. We divided the upland core into a soil zone above the fine-grained layer (<2.3 m) and a sediment zone below (>2.3 m). The swamp core was divided into soil and sediment zones at 2.3 m and into reduced and oxidized sediments at the color change at 6.1 m (Fig. 2). The oxidized surface layer of organic detritus is not included in the swamp soil zone. Results are presented for individual layers in depth profiles in Fig. 2 and Table 3 and for the designated zones of the cores as mean values and sample standard deviations (Table 2). The means and standard deviations are weighted by the thickness of the layer over which each value was obtained.

Clay-sized and Heavy Mineral Fractions Distribution and Composition

The clay-sized fractions contained mainly kaolinite, minor amounts of goethite and quartz, and trace amounts of muscovite. Ferrihydrite ($5Fe_2O_3 \cdot 9H_2O$), gibbsite ($Al(OH)_3$), and other Fe and Al oxide phases were not detected. Goethite (relative abundance represented by peak area ratio of goethite d_{110}/kaolinite d_{001}) was present in most layers of the upland core but absent from most layers of the swamp core above 6.1 m. Only the major goethite peak (d_{110} = 4.18 Å) was detectable in the clay-sized fraction. The d_{110} peak was broad and shifted to slightly smaller d-spacings (as low as 4.16 Å) in some samples, most noticeably in the upland soils and sediments.

The deeper upland sediments and swamp-oxidized sediments contained about 2–3 times as much clay-sized material as the swamp-reduced sediments. Clay-sized materials were about three times more abundant in the deeper upland sediments than in the upland soils, but swamp soils contained about twice as much clay-sized material as swamp-reduced sediments.

Organic matter was much more abundant in the swamp core, especially in the soil zone. The organic matter content of both cores generally decreased with depth. Organic matter and clay contents were high in the thin layers separating the soil and sediment zones, suggesting that these constituents were eluviated from the soil by infiltrating water and deposited in these layers.

The heavy mineral suite separated from five upland and six swamp layers consisted mainly of 50–200 μm subangular to rounded grains. Heavy mineral contents measured in these samples varied considerably with depth in both cores. Bromoform separations gave heavy mineral contents in the same range as those determined by point counting for different samples. XRD indicated that the heavy minerals are mainly pseudorutile, with minor amounts of ilmenite, rutile, zircon, and quartz, and trace amounts of augite. The presence of quartz was an artifact related to incomplete separation.

Soil and Sediment Elemental Composition

Surface Fe was much more abundant in the oxidized soils and sediments than in the reduced soils and sediments with the exception of the surface layer in the swamp, which contained the highest surface Fe content (Fig. 2). We suspect that Fe^{2+} diffusing up from the reduced soils was oxidized due to the presence of dissolved O_2. Fe^{2+} oxidation may have been accelerated by microbial action, as in the case of bog iron formation (CRERAR et al., 1979). Soils and sediments with high surface Fe were colored shades of yellow (corresponding to oxidized zones), while those with low surface Fe (≤ 5 μmol g^{-1}) were generally white to light gray (corre-

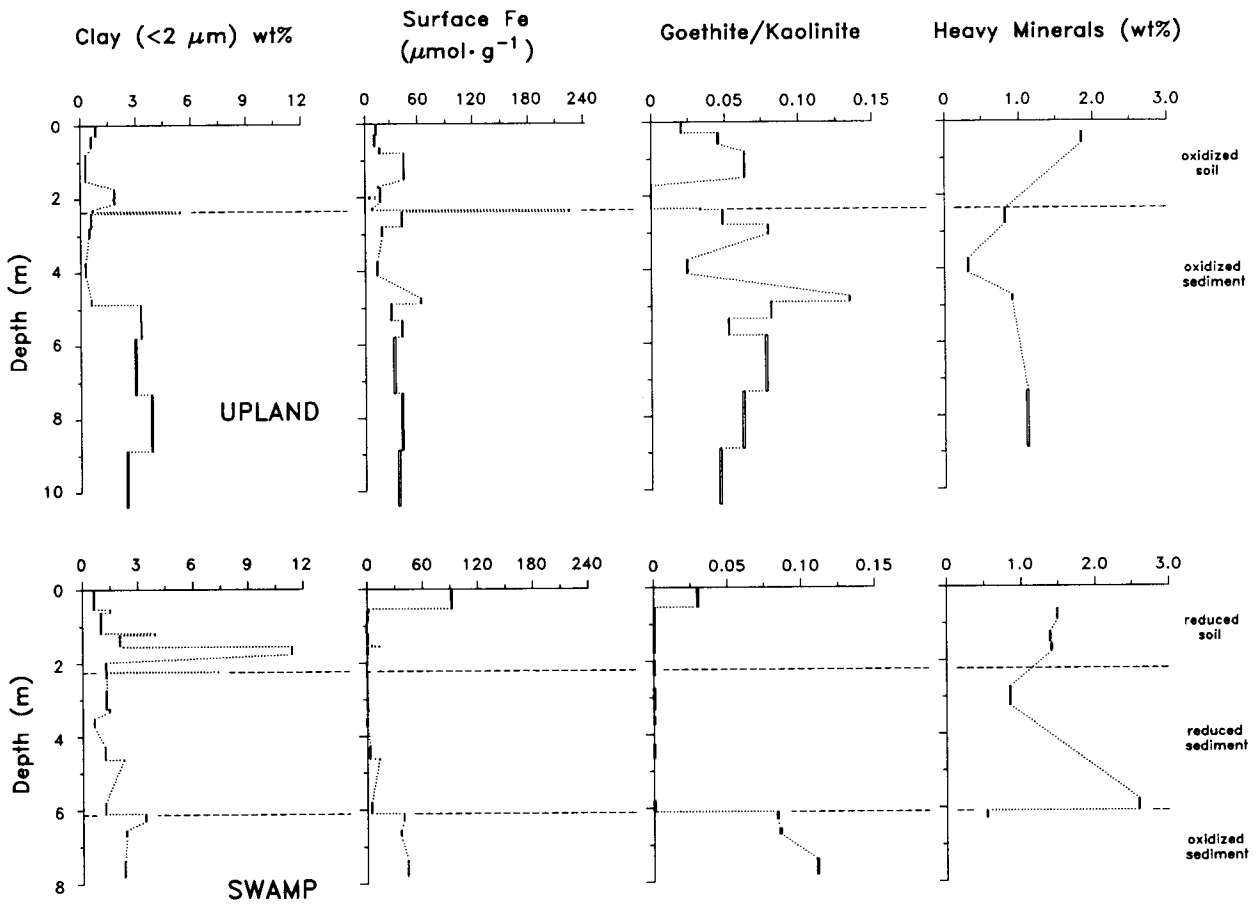

FIG. 2. Vertical profiles of element and mineral concentrations in upland (above) and swamp (below) cores: clay-sized (<2 μm) fraction; surface Fe; ratio of goethite d_{110} peak area/kaolinite d_{001} peak area from XRD; and heavy mineral fraction. Layer thicknesses are shown by solid vertical bars for samples taken by split-tube sampler and by open bars for samples taken from auger flights. Horizontal dashed lines show grouping of layers into soil and sediment zones for mean element and mineral contents presented in Table 2.

sponding to reduced zones). Surface Fe and goethite abundance are correlated in both cores ($R^2 = 0.70$, $n = 17$, upland; $R^2 = 0.64$, $n = 20$, swamp). Other less-crystalline Fe(III) oxides, such as ferrihydrite, may also comprise a small portion of the surface Fe.

The amount of surface Fe may have been overestimated by extraction of Fe from the Fe-Ti oxides in the heavy mineral fractions, particularly in the swamp soils and reduced sediments where goethite was not detected by XRD. Generally, for samples with high surface Fe content and goethite abundance, Fe removed from the heavy minerals probably comprised <2% of surface Fe, but for samples with low surface Fe and high heavy mineral contents (especially the reduced sediments in the swamp core), the heavy mineral contribution to surface Fe may comprise as much as 60% of the surface Fe measured (RYAN and GSCHWEND, 1991). Fe(III) in pseudorutile may be particularly susceptible to dissolution by the reducing solution.

Surface Al was >95% removed in the first extraction of all of the upland and swamp samples containing goethite. For samples that did not contain goethite, the amount of Al extracted did not significantly decrease with succeeding extractions, suggesting that Al was dissolved mainly from aluminosilicate minerals. High surface Al and Fe contents coincided with high organic matter in some thin soil layers in which goethite was not detected. In these cases, Al and Fe may have been associated with organic matter and removed by the selective extractions.

Total Fe was divided into two fractions, surface Fe and structural Fe, where structural Fe is the difference between total and surface Fe. The structural Fe estimates were used to represent the amount of Fe in the Fe-Ti oxides of the heavy mineral fraction because structural Fe correlated far better with the heavy mineral content ($R^2 = 0.53$; $n = 11$) than with other possible sources of Fe-bearing primary minerals (clay- and silt-sized fractions). We assumed that total Ti represented the amount of Ti in the Fe-Ti oxides because total Ti also correlated with heavy mineral content ($R^2 = 0.63$; $n = 11$). Thus, the ratio of structural Fe/total Ti (struct Fe/Ti) was considered to be a gauge of the overall composition of the ilmenite-pseudorutile-rutile suite that dominated the heavy mineral fraction. Corrections for the overestimation of surface Fe by dissolution of Fe-Ti oxides did not significantly change the structural Fe/Ti ratios in the samples for which heavy mineral content was measured. Subtle differences in structural Fe/Ti may be discerned

Table 2. Mean values and sample standard deviations (weighted by layer thicknesses) of clay, organic matter and total and surface elements in the Upland and Swamp cores.

	Upland		Swamp		
	oxidized soil	oxidized sediment	reduced soil	reduced sediment	oxidized sediment
depth range (m)	0 to 2.3	2.3 to 10.4	0 to 2.3	2.3 to 6.1	6.1 to 7.8
clay–sized (wt%)	0.8±0.6	2.6±1.1	2.3±3.2	1.2±0.3	2.6±0.5
goethite/kaol	0.04±0.03	0.06±0.02	0	0	0.10±0.01
surf Fe (μmol g^{-1})	23±14	34±8.3	1.5±1.6	3.0±2.5	42±3.5
surf Al (μmol g^{-1})	5.7±2.7	6.4±1.4	5.6±6.5	3.8±1.0	4.4±0.4
surf Al/Al+Fe	0.21±0.04	0.16±0.02	0.72±0.16	0.61±0.12	0.10±0.00
org matter (wt%)	1.4±2.2	0.2±0.1	5.0±7.2	0.4±0.1	0.2±0.1
total Fe (μmol g^{-1})	70±13	75±12	55±12	47±21	67±5.5
total Ti (μmol g^{-1})	100±23	79±14	120±28	96±43	39±7.8
total Al (μmol g^{-1})	820±210	830±170	690±180	700±49	580±100
struct Fe (μmol g^{-1})	47±12	41±7.4	53±12	44±19	25±6.2
struct Fe/Ti	0.47±0.05	0.52±0.05	0.44±0.02	0.47±0.04	0.66±0.11

between the oxidized and reduced sediments and between the soils and sediments in both cores, but the magnitude of the differences is similar to that of the uncertainties in the ratios.

Total Al was roughly 50–200 times as abundant as surface Al and was not correlated with surface Al, clay-sized, or heavy mineral content. Total Al concentrations matched the expected contributions of Al from feldspar, mica, kaolinite, and the heavy mineral fraction if we assumed that the portion of the coating and matrix volume determined by point counting in excess of the estimated volume of the clay-sized fraction (Table 1) was comprised of aluminosilicates (kaolinite or muscovite).

Scanning Electron Microscopy and Energy-Dispersive X-ray Spectroscopy

SEM examination of disoriented sediments showed that the quartz grain surfaces in the upland soil and sediments and the swamp-oxidized sediments were extensively covered by clay plates in the <5 μm size range. Occasionally, bridges between grains were preserved despite the disoriented nature of the samples (Fig. 3a). In the swamp soil and reduced sediments, grain surfaces were relatively free of coatings (Fig. 3b).

ESEM analysis of the uncoated thin sections revealed details regarding the nature of the coatings on quartz grain surfaces. We concentrated on the swamp sediments at the redox boundary at 6.1 m depth. In the swamp-oxidized sediment (S.8.2), pore spaces between quartz grains were commonly filled with fine-grained, densely packed material. In addition to matrix buildup in constricted pore spaces, grains were coated on surfaces exposed to open pore spaces (Fig. 4a). The coatings and matrix fillings did not show any preferential arrangement. The thickness of the coatings in the open pores varied from 0–10 μm thick, and in the constricted pores, the matrix fillings spanned thicknesses up to 100 μm. The grain coatings adjacent to the large pore spaces appeared to be comprised of clay plates in the ≤ 1 μm size range (Fig. 4b). In contrast, the swamp-reduced sediment (S.8.1) showed accumulation of clay in some restricted pore spaces (Fig. 4c), but open pores were predominantly free of coatings. The fine-grained material collected in the restricted pore spaces consisted mainly of elongated, fibrous minerals loosely jumbled on the quartz surface (Fig. 4d).

Element profiles across quartz grain coatings acquired by EDX (Fig. 5) revealed that coatings in the oxidized sediments (U.8.1 and S.8.2) contained far more Fe than those in the reduced sediment (S.8.1). Fe/Si ratios vary widely in the coatings, but the minimum Fe/Si in the oxidized sediments was still about four times greater than the maximum Fe/Si detected in the reduced sediment. If the 2–50 mole% Fe (where Fe concentration is reported as molar percentage of Fe relative to the total content of Fe, Al, Si, Ti, K, and Cl, but not O) was present entirely as goethite, and Al and Si are present as kaolinite, then goethite may comprise a range of 1.4–58 wt% of the coatings. The ratio of Al/Si ranged from 0.1–0.9 in the coatings, gradually reaching a plateau at approximately 0.8 at distances of 2–3 μm from the quartz grain surface. Low Al/Si ratios recorded at the quartz-coating interface probably reflect the averaging of Al and Si contents of quartz and kaolinite in the volume penetrated by the electron beam.

SEM/EDX analysis of the heavy minerals revealed primarily Fe- and Ti-rich mineral grains tentatively identified

Table 3. Element and mineral distributions and derived quantities for individual sample layers.

sample	depth (m)	organic matter (wt%)	surf Al	total Fe	total Ti	total Al	struct Fe	struct Fe/Ti	surf Al/(Al+Fe)
			———		μmol g^{-1}	———			
Upland									
U.1.1	0.00–0.30	3.7	3.6	81	150	1100	70	0.48	0.24
U.1.2	0.30–0.61	0.32	2.3	69	110	980	59	0.55	0.18
U.2.1	0.65–0.80	7.3	6.1	61	89	720	46	0.51	0.28
U.2.2	0.80–1.52	0.21	8.9	81	96	590	39	0.41	0.18
U.3.1	1.70–1.73	5.9	5.1	67	100	680	53	0.51	0.27
U.3.2	1.73–1.98	0.14	4.8	53	75	900	37	0.49	0.23
U.3.3	1.98–2.03	0.70	2.2	36	58	1100	32	0.55	0.33
U.3.2	2.03–2.13	0.14	4.8	53	75	900	37	0.49	0.23
U.4.1	2.29–2.34	0.31	1.9	44	80	650	37	0.46	0.21
U.4.2	2.34–2.39	1.3	35	340	78	1100	120	1.54	0.14
U.4.3	2.39–2.79	0.30	9.3	99	120	1200	60	0.49	0.19
U.5.1	2.79–3.05	0.08	3.2	52	71	1000	34	0.49	0.16
U.6.1	3.73–4.11	0.12	2.5	49	67	1000	37	0.55	0.17
U.7.1	4.72–4.88	0.19	8.8	88	41	790	28	0.69	0.13
U.8.1	4.88–5.33	0.22	6.5	67	74	750	40	0.54	0.19
U.9.1	5.33–5.8	0.13	6.1	77	88	870	38	0.43	0.13
U.10.1	5.8–7.3	0.12	6.3	66	74	900	35	0.48	0.17
U.11.1	7.3–8.8	0.45	7.2	77	72	860	48	0.52	0.15
U.12.1	8.8–10.4	0.17	6.1	85	86	590	49	0.58	0.15
Swamp									
S.1.1	0.00–0.53	17	30	150	110	560	57	0.53	0.24
S.1.2	0.53–0.61	1.8	3.6	52	120	480	49	0.40	0.56
S.1.3	0.61–0.91	0.68	1.4	46	98	620	44	0.45	0.47
S.2.1	0.91–1.19	0.18	3.8	50	110	670	49	0.44	0.85
S.2.2	1.19–1.24	0.50	3.8	52	120	730	51	0.41	0.74
S.2.3	1.24–1.52	0.67	3.8	59	150	660	58	0.39	0.72
S.3.2	1.55–1.57	5.3	8.9	71	130	620	57	0.43	0.38
S.3.3	1.57–1.78	1.2	21	81	180	1200	80	0.45	0.94
S.4.1	1.98–2.24	0.46	2.6	44	96	740	43	0.45	0.76
S.4.2	2.24–2.26	2.0	16	55	100	1200	51	0.49	0.81
S.4.1	2.26–2.39	0.46	2.6	44	96	740	43	0.45	0.76
S.5.1	2.74–3.25	0.38	3.4	33	68	670	32	0.47	0.72
S.5.2	3.25–3.33	0.47	3.8	41	78	860	39	0.50	0.66
S.6.1	3.51–3.73	0.16	2.4	28	49	690	27	0.55	0.70
S.7.1	4.27–4.62	0.38	4.4	45	96	670	41	0.43	0.51
S.7.2	4.62–4.65	0.57	8.3	86	150	870	72	0.48	0.37
S.8.1	5.79–6.10	0.29	4.7	86	180	710	80	0.45	0.45
S.8.2	6.10–6.30	0.38	4.0	59	26	750	20	0.79	0.09
S.9.1	6.55–6.71	0.14	4.1	75	48	560	37	0.78	0.10
S.10.1	7.37–7.80	0.13	4.8	68	41	500	23	0.56	0.10

as pseudorutile, ilmenite, and rutile (based on Fe/Ti_{edx}), as well as trace amounts of grains that contained Mg, Al, Si, and Ca. The trace minerals may have included augite and sphene ($CaTiSiO_5$). Fe-Ti oxide grains with Fe/Ti_{edx} ratios closest to the ideal ratio of pseudorutile, Fe/Ti = 0.67, were most abundant in the samples. Rutile grains ($Fe/Ti_{edx} \leq 0.1$) were larger and more rounded than the pseudorutile grains. The surfaces of pseudorutile grains in each of the soil and sediment samples showed signs of advanced weathering in the form of etch pits, cracks, and generally degraded surfaces. EDX profiles across Fe-Ti oxide grains showed that surfaces were depleted in Fe relative to Ti compared to interiors (surface Fe/Ti_{edx} = 0.33 to 0.49; interior Fe/Ti_{edx} = 0.47 to 0.76). The difference between surface and interior Fe/Ti_{edx} was greater in the oxidized sediments (S.8.2, U.8.1). The structural Fe/Ti ratios estimated for these samples fell between the surface and interior Fe/Ti_{edx} ratios, indicating that the structural Fe/Ti ratio determined by chemical means provided an accurate overall Fe/Ti ratio reflecting mainly structural Fe and Ti in the Fe-Ti oxides in the heavy mineral fraction.

DISCUSSION

Evidence of Colloidal Clay Transport

Two lines of evidence support our contention that clay colloids have been and, under some conditions, are still transported by groundwater flow in the Cohansey Sand. First, clay appears to have been delivered into the sand layers of the Cohansey after deposition. Second, suspended clay can currently be found in zones of anoxic groundwater (RYAN and GSCHWEND, 1990).

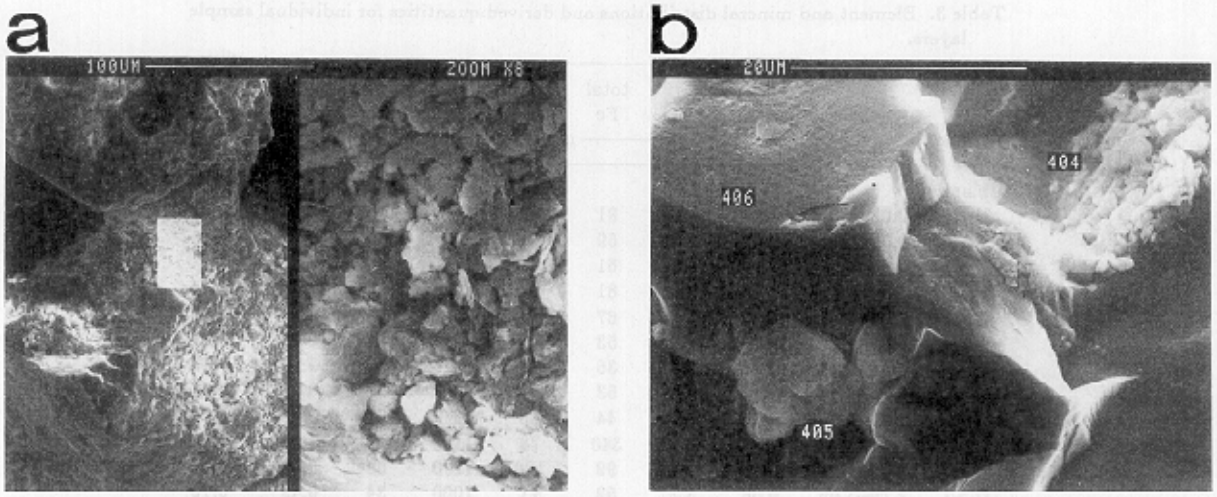

FIG. 3. SEM photographs of quartz grain surfaces in swamp-oxidized sediment (sample S.8.2) and swamp-reduced sediment (sample S.8.1). Scale bars show dimension. (a) Sample S.8.2: kaolinite particles completely coating quartz surfaces and bridging distance between grains (left); kaolinite packed into the bridge in a manner characteristic of colloidally transported clay (right; 8× zoom of bright region at left). (b) Sample S.8.1: quartz surface relatively free of kaolinite particles; the few kaolinite particles attached are located in protected cracks and corners of the angular quartz grains. Numbers refer to EDX spectra not shown.

The anisopachous, randomly oriented, mineralogically heterogeneous coatings of kaolinite and Fe(III) oxides appear to have been formed by accumulation of kaolinite particles from flowing groundwater, based on criteria applied by MATLACK et al. (1989) and MORAES and DE ROS (1990). Interbedded clay-silt laminations, from which infiltrating water may have eluviated kaolinite particles into underlying sand layers, are likely sources of clay. The overlying source of clay for these sediments may have been removed by erosion. Detrital or authigenic origins of kaolinite particles in the Cohansey Sands are unlikely. The wave- and wind-winnowed sand sheets of the Cohansey Sand were deposited relatively free of detrital clay-sized particles (CARTER, 1978). Sources of authigenic clay, primarily feldspars, are scarce in the Cohansey because very little feldspar was deposited in the Cohansey Sand (RHODEHAMEL, 1979a). Furthermore, kaolinite coatings are evenly distributed throughout the sediments and not concentrated near aluminosilicate parent grains.

Clay observed in the Cohansey Sand has been attributed to vertical transport in the unsaturated zone ("illuviation" or "mechanical infiltration"). OWENS et al. (1983) found halloysite in upper layers of the Cohansey only in locations where it was overlain by the Late Miocene Bridgeton Formation, in which halloysite is common. Infiltrated clay has also been observed in halos that mark the former menisci of perched water above small, impermeable clay lenses (W. L. Newell, USGS, Reston, VA, pers. comm., 1991). In contrast, the mobilization of kaolinite colloids in the anoxic groundwater below the swamp suggests that kaolinite is being transported in the saturated zone as well as in the unsaturated zone.

In the saturated zone, colloids are operationally defined as particles that remain suspended and are mobile at groundwater flow rates. Colloids remain suspended by avoiding collisions with framework grains that result in attachments. The collision frequency depends on particle size and flow velocity. At typical groundwater velocities, collisions of particles < 0.1 μm are mainly caused by Brownian diffusion; for particles > 1 μm, collisions are caused primarily by sedimentation (YAO et al., 1971). Particles in the 0.1–1 μm size range experience the fewest collisions. Kaolinite colloids observed in the swamp groundwater (RYAN and GSCHWEND, 1990) and kaolinite particles attached to quartz grains are generally in the <2 μm size range, so the expected collision frequency of these particles is relatively low. We estimate that a particle of 0.5 μm diameter experiences only one collision for every five grains passed, using a groundwater velocity of 10^{-4} cm s^{-1}, temperature of 15°C, average grain diameter of 250 μm, and particle thickness of 50 nm in the analytical equations developed by YAO et al. (1971).

The probability of an attachment of a colloid to a collector grain following a collision is controlled by attractive and repulsive forces acting between the colloid and grain surfaces. We estimated the total potential energy of interaction between colloid and grain as the sum of Born repulsion, van der Waals attraction, and electrostatic repulsion between spherical colloid and grain as a function of distance. Born repulsion was calculated using the expression derived by RUCKENSTEIN and PRIEVE (1976) with a collision diameter $\sigma = 8$ Å, colloid radius of 0.4 μm, and grain radius of 250 μm. The van der Waals energy was calculated using the expression derived by VERWEY and OVERBEEK (1948) with a Hamaker constant of $A = 1.7 \cdot 10^{-20}$ J (HOUGH and WHITE, 1980). Electrostatic repulsion was calculated using the expression derived by HOGG et al. (1966) with ionic strength of 260 μM, kaolinite surface potential of −0.11 V determined by electrophoretic mobility (RYAN and GSCHWEND, 1990), and quartz surface potential estimated at −0.20 V from electrophoretic mobility data of KIA et al. (1987) at pH 4.6. With these assumptions and parameter values, we estimated that an energy barrier of 55 $\mathbf{k}T$ (where k is the Boltzmann constant and T is absolute temperature) inhibits the attachment of kaolinite colloids to quartz grains in the swamp groundwater. The magnitude of

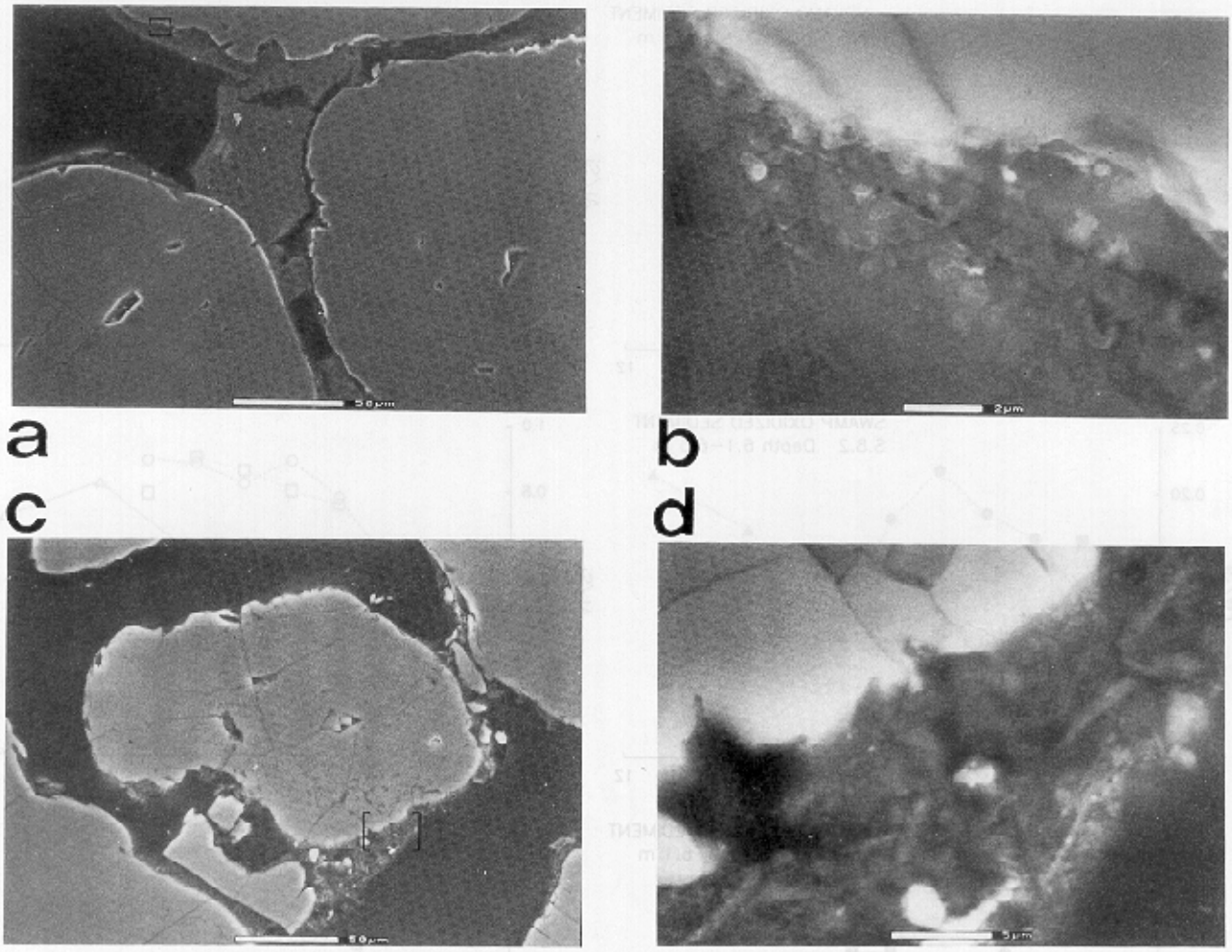

FIG. 4. Environmental SEM photographs of polished, oriented thin sections of oxidized sediment (sample S.8.2) and reduced sediment (sample S.8.1) from the swamp core. Photographs arranged properly with respect to the orientation of the sediments in the cores. Scale bars show dimension. Sample S.8.2: (a) coatings in open pores and matrix fillings between quartz grains; (b) coating composed of particles resembling clay plates in enlargement of enclosed area in (a). Sample S.8.1: (c) retention of clay particles in restricted pore space between quartz grains. Open pore surfaces, more exposed to groundwater flow, are uncoated. (d) Coatings contain loosely packed, larger, elongated clay particles in enlargement of enclosed area in (c).

this energy barrier corresponds to very low attachment probability. With low collision frequency and low attachment probability, the observed mobility of kaolinite colloids in the swamp groundwater (pH = 4.5) seems feasible.

Role of Fe(III) Oxides in Clay Transport

The energy barrier inhibiting attachment of kaolinite to quartz is estimated to be larger (78 kT) in the oxic upland groundwater (pH = 4.8) due to higher surface potentials, but colloids are essentially absent in the water (RYAN and GSCHWEND, 1990). We hypothesized that the barrier to attachment had been removed by the accumulation of Fe(III) oxides on the quartz surfaces because (1) Fe(III) oxides are positively charged at the groundwater pH ($pH_{zpc} \cong 7.0$–8.5; PARKS, 1967), and (2) silica surface charge can be reversed from negative to positive by adsorption of metal ions (JAMES and HEALY, 1972). We expected that correlations between clay and surface Fe contents would illustrate the role of Fe(III) oxides in the attachment of kaolinite colloids.

The relationship between the surface Fe and clay content of the sediment layers highlights three groups of sediments (Fig. 6): (1) high surface Fe and clay in the deeper oxidized sediments in both cores, (2) low surface Fe and clay in the reduced sediments, and (3) high surface Fe and low clay in the oxidized sediments just below the soil zone in the upland core. If the four upland sediment layers of the third group are dismissed on the basis that soil zone processes diminished the supply of clay to these layers, surface Fe, and clay content are correlated ($R^2 = 0.74$; $n = 15$). However, clay content remained substantial even when surface Fe content was very low. The residual clay content (about 1.0 wt%) indicates that the surface Fe-clay relationship reflects the amount of kaolinite detached and mobilized after the Fe(III) oxide cement is dissolved, rather than the amount of kaolinite attached to Fe(III) oxides. The residual clay may represent kaolinite released by Fe(III) oxide dissolution and trapped in restricted

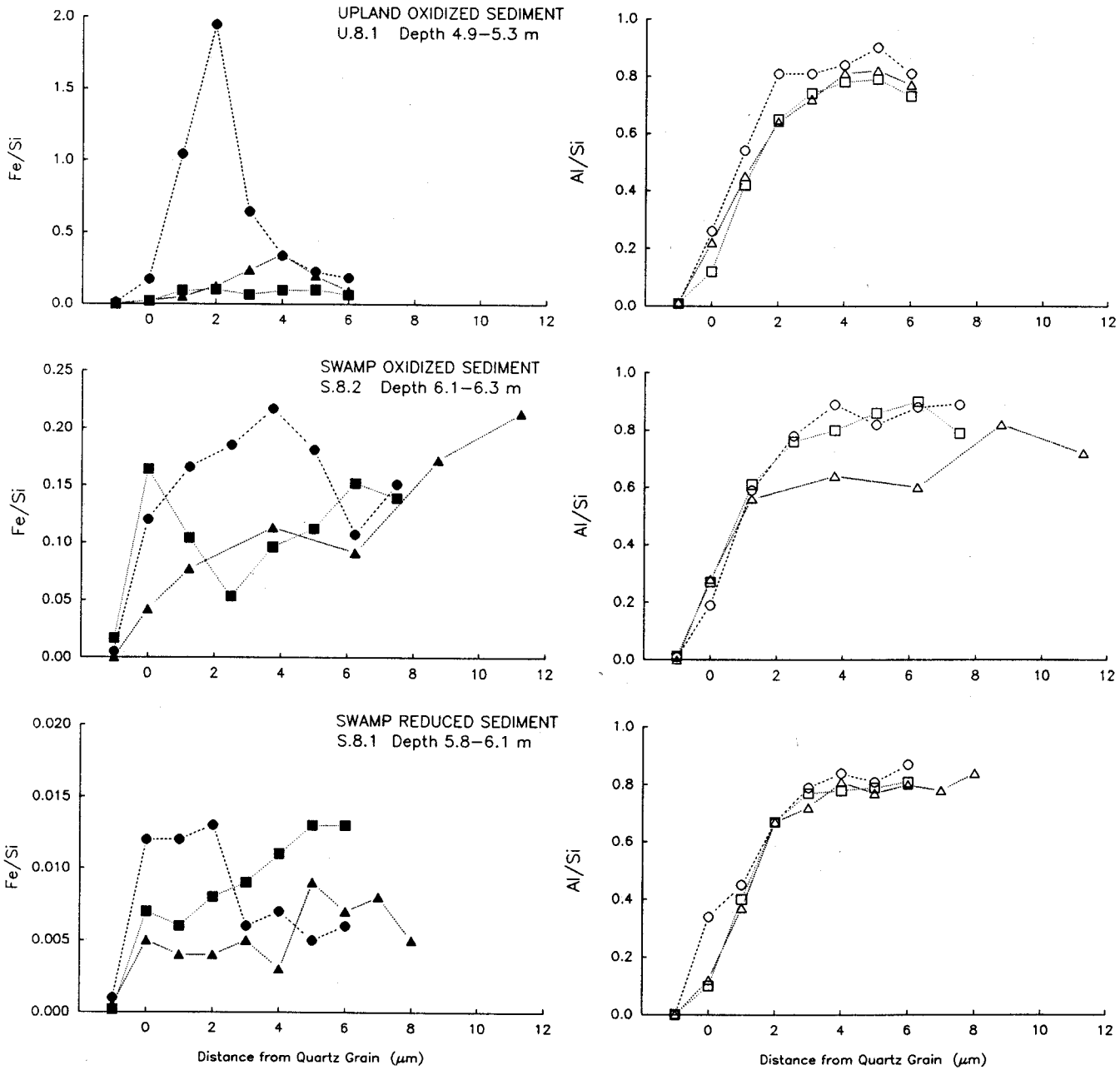

FIG. 5. Element profiles across kaolinite-Fe(III) oxide coatings on quartz grains in upland oxidized sediment (U.8.1), swamp oxidized sediment (S.8.2), and swamp reduced sediment (S.8.1) obtained by spot EDX analyses in Au-coated thin sections. Connected data points represent profiles across three different grain coatings in each sample.

pore spaces. Alternatively, small amounts of Fe(III) oxides may remain in the restricted pores (Fig. 5) cementing the residual kaolinite particles.

The removal of suspended kaolinite by goethite coatings must require a continuous supply of Fe to maintain the positive surface charge of the framework grains. Without constant Fe supply, the attachment of a kaolinite layer would result in a return to repulsive interactions between colloid and grain surfaces as colloids encountered a colloid-coated grain (42 kT energy barrier at pH 4.8). EDX analyses showed that Fe is distributed throughout the coatings (Fig. 5), suggesting that Fe has been continually supplied to grain surfaces. The source of the Fe is the slow, ongoing dissolution of the Fe-Ti oxides, ilmenite and pseudorutile.

Release of Iron from Fe-Ti Oxides

The major Fe-bearing primary minerals in the Cohansey sediments are pseudorutile ($Fe_2O_3 \cdot TiO_2$) and ilmenite ($FeO \cdot TiO_2$). The XRD results, structural Fe/Ti, and Fe/Ti_{edx} indicate that most of the ilmenite has been converted to pseudorutile, releasing Fe^{3+} to solution. Pseudorutile is

formed only as an intermediate weathering product of ilmenite under oxidizing conditions (TEUFER and TEMPLE, 1966). Ilmenite alteration to pseudorutile is slow (TEMPLE, 1966) because it involves the solid-state oxidation of Fe(II) in ilmenite and diffusion of one-third of the resulting Fe(III) out of the structure to maintain charge balance:

$$3\ FeO \cdot TiO_2 \rightarrow Fe_2O_3 \cdot 3TiO_2 + Fe^{3+} + 3e^-.$$

The Cohansey sediments were probably oxidized following subaerial exposure about 5 million years ago (RHODEHAMEL, 1979a). It is unlikely that much Fe was released from ilmenite prior to the onset of oxidizing conditions in the sediments. Ilmenite is congruently dissolved under acidic, reducing conditions, producing Fe^{2+} and authigenic TiO_2 (TEMPLE, 1966; GREY and REID, 1975), but we did not find any authigenic TiO_2 in these sediments. The porewaters of the Cohansey sediments were probably reducing and alkaline during the 15 million years that the sediments were submerged. Thus, most of the Fe released in the Cohansey sediments has come from the alteration of ilmenite to pseudorutile over the past 5 million years. Minor amounts of Fe may also have been derived from the complete dissolution of Fe-bearing silicates (amphiboles, pyroxenes) and aluminosilicates (augite) that are no longer present in the sediments, but these minerals were apparently never present in significant amounts in the initial deposits (MARKEWITZ, 1969; RHODEHAMEL, 1979a).

The structural Fe/Ti and Fe/Ti_{edx} in the soils and reduced sediment are slightly lower than those in the oxidized sediments, suggesting that acidic, reducing conditions that developed in the soils and below the swamp perhaps as recently as 10,000 years ago probably promoted the removal of Fe(III) from pseudorutile surfaces following adsorption of reduced species and protons. Signs of more advanced weathering in the reduced sediments and soils were not evident in SEM examination of the pseudorutile grain surfaces.

Iron Mobility in the Sediments

The fate of Fe released by the weathering of Fe-Ti oxides in the Cohansey Sand depends on the redox potential, pH, and complexing ligand concentration of the porewater. To determine whether Fe released from Fe-bearing primary minerals was deposited as secondary Fe(III) oxides in the same layer or transported away from the layer as dissolved Fe, we estimated the amounts of Fe deposited and released in each layer. Fe deposited was estimated using the surface Fe measurements. Fe released was estimated by assuming the following: (1) Fe originates entirely from the weathering of Fe-Ti oxides, (2) the Fe-Ti oxides were originally deposited as ilmenite, and (3) Ti is conserved in the parent grains during weathering of Fe-Ti oxides. Thus, the amount of Fe released by weathering is the difference between total Ti and structural Fe.

These calculations suggest that Fe released from the Fe-Ti oxides in the swamp soil and reduced sediments was removed by groundwater flow (Fig. 7). Fe released in acidic, reduced sediments is most likely present as soluble Fe^{2+} species, resulting in loss of Fe from the soil or sediment (ANAND and GILKES, 1984; MORAD and ALDAHAN, 1986). Fe in excess of intrastratal supply may have been deposited in the oxidized layers below 6.1 m by infiltrating water. Fe deposited in the surface soil layer of the swamp core may be delivered by diffusion of dissolved Fe from the reduced soil layers below.

In the upland core, Fe is removed from the soil zone and deposited in the thin layer at 2.3 m depth. In the upper sediments, Fe may have also been redistributed downward between 2.3 and 4.9 m. Below 4.9 m, Fe release and deposition are nearly balanced. However, even in the oxidized sediment layers in which Fe release and Fe deposition were roughly balanced, Fe^{3+} released by Fe-Ti oxide weathering was transported over at least pore-scale distances. Quartz grains were ubiquitously coated by kaolinite-Fe(III) oxide mixtures without regard to proximity to Fe-Ti oxide grains. The pore-scale transport of Fe in oxidized sediments implies that Fe^{3+} temporarily formed soluble complexes or colloidal Fe(III) oxides stabilized by organic coatings. Organic acid components of the dissolved organic matter (present at 120 μM C; RYAN and GSCHWEND, 1990) may have been the most important complexing ligands for complexing Fe^{3+}. CRERAR et al. (1981) determined that most of the dissolved Fe in Pine Barrens groundwater was associated with dissolved organic matter. Colloidal Fe(III) oxides have also been observed in Pine Barrens groundwater (LANGMUIR, 1969).

Formation of Surface Fe(III) Oxides

Geological observations of ilmenite weathering in oxidized sediments frequently report pseudomorphic replacement of parent ilmenite grains by hematite and rutile (GREY and REID, 1975), suggesting that rapid hydrolysis of Fe and Ti led to epitactic precipitation of Fe and Ti oxides. Instead of epitactic precipitation of hematite in oxidized sediments, we observed that Fe was transported away from the Fe-Ti oxides and spread uniformly throughout the sediments. The transport of Fe^{3+} away from the parent Fe-Ti oxides implies that Fe^{3+} activity was not sufficiently high to precipitate Fe(III) oxides on the parent Fe-Ti oxides. Because Fe(III) oxides were not precipitated even at the source of Fe, it is unlikely that porewaters would be supersaturated with respect to Fe(III) oxides near the surfaces of quartz grains distant from the source. MINEQL (WESTALL et al., 1976) calculations using groundwater chemistry data (RYAN and GSCHWEND, 1990; LORD et al., 1990) confirmed that the upland groundwater is undersaturated with respect to Fe(III) oxides (without including the effect of organic acid ligands, which would increase dissolved $[Fe^{3+}]$).

We suspect that Fe(III) oxides on quartz grains originated as adsorbed surface complexes. Silanol groups on quartz and amorphous silica surfaces strongly adsorb hydrolyzed Fe^{3+} species (DUGGER et al., 1964; SCHINDLER et al., 1976). Continued adsorption of successive layers of Fe^{3+} leads to formation of Fe oxyhydroxide surface deposits (ANDERSON et al., 1984; TAYLOR et al., 1990). Given the extensive coverage of quartz surfaces by kaolinite-goethite coatings, it is apparent that Fe^{3+} adsorption has not been limited to patches or surface imperfections on the quartz surface; instead, Fe^{3+} is present in significant quantities over a high percentage of quartz surfaces. The distribution of Fe throughout the coatings indicates that additional Fe^{3+} was adsorbed by the kaolinite particles following their attachment to previously accumulated Fe(III) oxides. Positively charged surfaces favorable for the continued removal of kaolinite from suspension could have been maintained in this way.

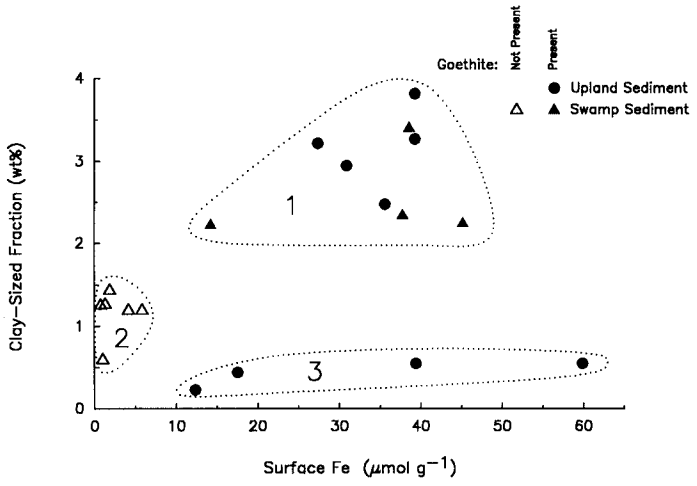

FIG. 6. Relationship of clay-sized content to surface Fe content for upland and swamp sediments. Sediment layers containing goethite marked by filled symbols. Enclosed areas represent (1) high surface Fe/high clay layers from oxidized sediments in both cores, (2) low surface Fe/low clay layers from reduced sediments in swamp core, and (3) high surface Fe/low clay layers from oxidized sediments just below soil zone in upland core.

Following the accumulation of Fe^{3+} on the quartz and kaolinite surfaces, goethite formation is favored over the formation of ferrihydrite or lepidocrocite (γ-FeOOH) in the Cohansey Sand because Fe(III) oxide nucleation is probably slow. Nucleation may be slowed by the following: (1) slow release of Fe^{3+} (GRAHAM et al., 1989) from the Fe-Ti oxides, (2) complexation of Fe^{3+} by organic acids (KÄMPF and SCHWERTMANN, 1982), and (3) slow oxidation of Fe^{2+} at low pH (SCHWERTMANN, 1988). Despite slow nucleation, goethite crystal size appeared to be limited to $\ll 1$ μm in most quartz coatings, possibly by the continuous attachment of kaolinite. Larger, discrete Fe(III) oxide crystals with the lath-like appearance of goethite formed only in locations where Fe concentration exceeded 10 mole%, or about 13 wt% FeOOH (if all Fe was present as goethite).

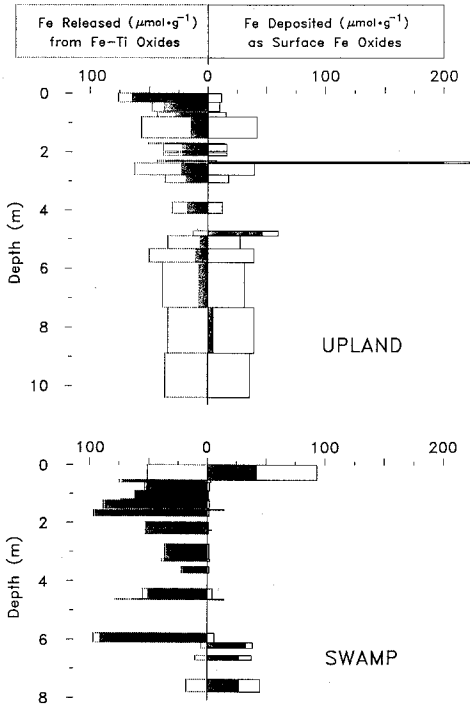

FIG. 7. Balance between Fe released by weathering of Fe-Ti oxides and deposition of secondary Fe(III) oxides in individual layers. Open bars with dotted horizontal lines on negative x axis show Fe released from ilmenite and pseudorutile; open bars with solid horizontal lines on positive x axis show surface Fe measured. Filled bars show difference between Fe weathered and Fe deposited as surface Fe. Net Fe export from a layer is shown as a negative difference; net Fe import to a layer is shown as a positive difference.

Goethite in the Cohansey Sand appeared to be considerably substituted by Al, as indicated by correlation of surface Fe and Al contents of sediment layers containing goethite ($R^2 = 0.65$; $n = 18$), shifts in the goethite d_{110} peaks to slightly smaller d-spacings in some samples (SCHULZE, 1984), and the lack of any Al oxyhydroxide phase in the sediments. The extent of Al substitution in goethite was estimated by the ratio of surface Al/(surface Fe + surface Al) in each layer (weighted mean values in Table 2). Goethite in the unsaturated upland soil had the highest proportion of AlOOH (20 mole%), perhaps due to lower H_2O activity (TARDY and NAHON, 1985). In the saturated sediments, goethite is less substituted by Al (upland sediment, 16 mole% AlOOH; swamp-oxidized sediment, 9.6 mole% AlOOH). The difference between Al substitution of sediment goethites may be caused by transport of excess Fe into the swamp-oxidized sediments from the overlying reduced sediments, resulting in higher ratios of dissolved Fe/Al. Thermodynamic stability calculations indicate that Al substitution increases goethite stability relative to hematite (TARDY and NAHON, 1985).

Kinetics of Fe(III) Oxide Dissolution and Clay Mobilization

If kaolinite is cemented to quartz surfaces by Fe(III) oxides, the kinetics of kaolinite release must be linked to the kinetics of Fe(III) oxide dissolution. Because Fe is distributed throughout the kaolinite coatings, kaolinite remobilization should commence at the onset of Fe(III) oxide dissolution

and continue until Fe(III) oxide is completely dissolved given suitably dispersive conditions of pH and ionic strength. HARRIS et al. (1987) envisioned a similar decementation process leading to vertical redistribution of clays in Fe(III) oxide-cemented soils in Florida. In the anoxic groundwater below the swamp, the goethite cementing phase is probably dissolved by reduction using organic carbon (represented by CH_2O) as an electron source:

$$FeOOH + \tfrac{1}{4}\,CH_2O + 2\,H^+ \rightarrow Fe^{2+} + \tfrac{1}{4}\,CO_2 + \tfrac{7}{4}\,H_2O.$$

A minimum of 12.5 pore volumes of infiltrating water are necessary to dissolve the goethite within a volume of sediment, assuming that (1) the sediments underlying the swamp originally contained 35 μmol g^{-1} surface Fe as goethite, (2) the sediment bulk density is 1.8 g cm^{-3} and porosity is 0.3, (3) the total organic carbon concentration in the water was 4 mM C, and (4) the reaction proceeds to completion in each pore volume. In (4), it is assumed that goethite dissolution is fast relative to the flushing of a pore volume. However, goethite dissolution may be slowed by low surface area (blocking of active sites by attached kaolinite) and reductants that are not extensively adsorbed or that do not transfer their electrons efficiently. With the hydraulic gradient measured between the swamp shallow and deep wells (0.17 $m \cdot m^{-1}$) and a representative range of hydraulic conductivities (10^{-2} to 10^{-4} cm s^{-1}, RHODEHAMEL (1979b)), a minimum of 50–5000 years is required to dissolve goethite in the 6 m of reduced sediment below the swamp. This estimate assumes that our rudimentary knowledge of local groundwater flow adequately describes the actual flow, both now and in the past. Nevertheless, it appears reasonable that a reduced zone of 6 m depth may have formed in the 10,000 years following glacial retreat.

The kinetics of Fe(III) oxide dissolution and clay release may be important in considering the environmental importance of decementation. The swampy terrain around McDonalds Branch could be considered a natural analog of a waste site that generates reducing leachates capable of dissolving Fe and Mn oxides. Plumes of reducing leachate have been reported to alter sediment color from yellow and brown to white and grey over periods of tens of years in sediments similar to the Cohansey Sand (KIMMEL and BRAIDS, 1980; NICHOLSON et al., 1983). In addition to the potential for clay colloid mobilization, trace metals (BAEDECKER and BACK, 1979) and colloidal organic matter (e.g., humic substances) adsorbed to oxide phases would be released following oxide dissolution. The potential mobilization of trace metals, organic matter, and clay particles in reducing plumes produces two deleterious effects: (1) the concentration of suspended colloids increases, enhancing the potential for colloid-facilitated transport of contaminants, and (2) the adsorptive capacity of the sediment decreases, diminishing the retardation of contaminants. Colloid mobilization by reducing plumes may be a widespread problem because sandy, Fe(III) oxide-coated sediments are common along the entire Atlantic Coastal Plain. Colloidal phases can also be mobilized by changes in groundwater chemistry in sediments cemented by other secondary mineral phases (carbonates, silica, evaporites). GSCHWEND et al. (1990) reported that silicate colloids were mobilized in a carbonate-cemented aquifer where they suspected that an increase in P_{CO_2} had dissolved calcite cement.

Implications for Clay and Iron Diagenesis

Clay infiltration is considered an unsaturated zone process (WALKER, 1976; PASSARETTI and ESLINGER, 1987); thus, the occurrence of infiltrated clay in sediments is cited as evidence for arid climates, deep water tables, and vertical redistribution of clay minerals early in the diagenetic sequence (WALKER et al., 1978; OWENS et al., 1983; MOLENAAR, 1986; MATLACK et al., 1989; MORAES and DE ROS, 1990). Much of the clay in the Cohansey Sand was probably emplaced by unsaturated zone infiltration during times of low sea level and deep water tables. However, our observations of the Cohansey Sand demonstrate that clays may be redistributed in saturated sediments as well. Horizontal redistribution of colloids is often important in the saturated zone as colloids follow the direction of groundwater advection. For example, SHORT et al. (1988), BUDDEMEIER and HUNT (1988), and PENROSE et al. (1990) each reported lateral transport of colloid-associated radionuclides away from their sources. Clay mobilization in saturated sediments has also been caused by reductions in ionic strength at sea water–fresh water interfaces (GOLDENBERG et al., 1983), resulting in horizontal movement of colloids in response to changes in sea level. Thus, evidence of colloidal clay morphologies and textures in sediments is not a certain indicator of unsaturated zone infiltration.

The development of red beds by intrastratal dissolution of unstable Fe-bearing primary minerals and subsequent precipitation of hematite is often considered to be an indicator of arid and tropical environments (WALKER, 1967; 1974). In this research, we have observed another example of intrastratal weathering of Fe-bearing primary minerals leading to the formation of secondary Fe(III) oxides in temperate climates. Goethite, the stable Fe(III) oxide in low-temperature, saturated surface sediments (TARDY and NAHON, 1985) is transformed to hematite through dehydration initiated by a decrease in H_2O activity following sediment uplift or an increase in temperature following sediment burial (BERNER, 1969; LANGMUIR, 1971). Sediments containing Fe(III) oxide-coated skeletal grains have also been observed in other temperate climates (SCHLUGER and ROBERSON, 1975; POSTMA and BROCKENHUUS-SCHACK, 1987).

CONCLUSIONS

Based on our observations and those of others who have investigated this Atlantic Coastal Plain deposit, we surmise that the diagenesis of Fe and clay in the Cohansey Sand followed this sequence of events. As initially deposited about 20 million years ago, the Cohansey Sand contained predominantly quartz and ilmenite grains in sheets of sand intercalated by clay- and silt-rich laminations. The marine sediments were presumably reducing and slightly alkaline, thus ilmenite remained relatively unweathered. Oxidizing and acidic conditions developed in the sediments upon emergence from the sea about 5 million years ago. Ilmenite weathered to pseudorutile under oxidizing conditions and slowly released Fe to the sediments. Fe^{3+} released by Fe-Ti oxide weathering spread over pore-scale distances throughout the sediment.

The quartz surfaces adsorbed Fe^{3+}, which accumulated on the surfaces primarily as microcrystalline, Al-substituted (9.6–20 mole% AlOOH) goethite. The accumulation of Fe(III) oxides eventually reversed the surface charge of the grains from negative to positive. As the water table deepened due to declining sea level, infiltrating water passed through clay-bearing layers and carried kaolinite particles downward into the sediments. The kaolinite was removed from suspension by attachment to the Fe(III) oxides on quartz surfaces through electrostatic attraction. Coatings on quartz grains accumulated to thicknesses of up to 10 μm and consist of goethite, and perhaps other less crystalline ferric oxides, intimately mixed with kaolinite. Conditions favorable for kaolinite attachment were maintained by the continued release of Fe from the Fe-Ti oxide weathering. The influx of organic matter–rich water from the swamp, beginning about 10,000 years ago, dissolved Fe(III) oxide coatings and released kaolinite particles, leading to the difference in clay content we observed between the swamp-reduced sediments and the oxidized sediments of the upland and swamp cores. Acidic, reducing conditions accelerated the weathering of the Fe-Ti oxides in the soils and reduced sediments as revealed by surface and interior Fe/Ti ratios measured by EDX.

Given the widespread occurrence of Fe(III) oxide-coated sands, especially on the Atlantic Coastal Plain, the mobilization of kaolinite particles by dissolution of Fe(III) oxide cement may be a significant process affecting clay and Fe diagenesis and colloid-facilitated transport. The mobilization and lateral transport of clay in response to changes in pore-water chemistry in saturated sediments suggests alternative interpretations of "illuviated" or "mechanically infiltrated" clay morphologies in sediments. The redistribution of Fe from sparsely distributed ilmenite and pseudorutile grains to secondary Fe(III) oxide coatings spread throughout the sediments further supports the contention that precursor red beds can be formed in temperature climates. Finally, changes or gradients in groundwater chemistry may incur decementation and clay mobilization, leading to colloid-facilitated transport of low-solubility species.

Acknowledgments—The authors are grateful to Pat Johnsson and Julia Barringer, USGS, West Trenton, NJ, and Christian Bethmann, Superintendent, Lebanon State Forest, NJ, for access to the sampling site; to Harry Hemond of MIT for the drill rig and a manuscript review; to John MacFarlane for graphics accompanying this paper and assistance during drilling; to Jonathan Clapp for assistance during drilling; to Mike Frongillo, MIT Center for Materials Science and Engineering, for ESEM operation; to Larry Poppe, USGS, Woods Hole, MA, for XRD guidance; to Dieke Postma for a constructive review of the manuscript; and to Frank Wobber, Subsurface Science Program, US Department of Energy, for financially supporting this research under contracts DE-FG02-86ER60413 and DE-FG02-89ER60846.

Editorial handling: E. J. Reardon

REFERENCES

ANAND R. R. and GILKES R. J. (1984) Weathering of ilmenite in a lateritic pallid zone. *Clays Clay Mineral.* **32,** 363–374.

ANDERSON M. A., PALM-GENNEN M. H., RENARD P. N., DEFOSSE C., and ROUXHET P. G. (1984) Chemical and XPS study of the adsorption of iron (III) onto porous silica. *J. Colloid Interface Sci.* **102,** 328–336.

BAEDECKER M. J. and BACK W. (1979) Modern marine sediments as a natural analog to the chemically stressed environment of a landfill. *J. Hydrol.* **43,** 393–414.

BERNER R. A. (1969) Goethite stability and the origin of red beds. *Geochim. Cosmochim. Acta* **33,** 267–273.

BROWNAWELL B. J. and FARRINGTON J. W. (1986) Biogeochemistry of PCBs in interstitial waters of a coastal marine sediment. *Geochim. Cosmochim. Acta* **50,** 157–169.

BUDDEMEIER R. W. and HUNT J. R. (1988) Transport of colloidal contaminants in groundwater: Radionuclide migration at the Nevada Test Site. *Appl. Geochem.* **3,** 535–548.

CARTER C. H. (1978) A regressive barrier and barrier-protected deposit: Depositional environments and geographic setting of the Late Tertiary Cohansey Sand. *J. Sediment. Petrol.* **48,** 933–950.

CRERAR D. A., KNOX G. W., and MEANS J. L. (1979) Biogeochemistry of bog iron in the New Jersey Pine Barrens. *Chem. Geol.* **24,** 111–136.

CRERAR D. A., MEANS J. L., YURETICH R. F., BORCSIK M. P., AMSTER J. L., HASTINGS D. W., KNOX G. W., LYON K. E., and QUIETT R. F. (1981) Hydrogeochemistry of the New Jersey Coastal Plain 2. Transport and deposition of iron, aluminum, dissolved organic matter, and selected trace elements in stream, ground-, and estuary water. *Chem. Geol.* **33,** 23–44.

DEGUELDRE C., BAEYENS B., GOERLICH W., RIGA J., VERBIST J., and STADELMANN P. (1989) Colloids in water from a subsurface fracture in granitic rock, Grimsel Test Site, Switzerland. *Geochim. Cosmochim. Acta* **53,** 603–610.

DUGGER D. L., STANTON J. H., IRBY B. N., MCCONNELL B. L., CUMMINGS W. W., and MAATMAN R. W. (1964) The exchange of twenty metal ions with the weakly acidic silanol group of silica gel. *J. Phys. Chem.* **68,** 757–760.

ENFIELD C. G. and BENGTSSON G. (1988) Macromolecular transport of hydrophobic contaminants in aqueous environments. *Ground Water* **26,** 71–79.

GIBLIN A. M., BATTS B. D., and SWAINE D. J. (1981) Laboratory simulation studies of uranium mobility in natural waters. *Geochim. Cosmochim. Acta* **45,** 699–709.

GOLDENBERG L. C., MAGARITZ M., and MANDEL S. (1983) Experimental investigation on irreversible changes of hydraulic conductivity on the seawater-freshwater interface in coastal aquifers. *Water Resources Res.* **19,** 77–85.

GRAHAM R. C., WEED S. B., BOWEN L. H., and BUOL S. W. (1989) Weathering of iron-bearing minerals in soils and saprolite on the North Carolina Blue Ridge front: I. Sand-size primary minerals. *Clays Clay Min.* **37,** 19–28.

GREY I. E. and REID A. F. (1975) The structure of pseudorutile and its role in the natural alteration of ilmenite. *Amer. Mineral.* **60,** 898–906.

GSCHWEND P. M., BACKHUS D. A., MACFARLANE J. K., and PAGE A. L. (1990) Mobilization of colloids in groundwater due to infiltration of water at a coal ash disposal site. *J. Contam. Hydrol.* **6,** 307–320.

HARRIS W. G., CARLISLE V. W., and CHESSER S. L. (1987) Clay mineralogy as related to morphology of Florida soils with sandy epipedons. *Soil Sci. Soc. Amer. J.* **51,** 1673–1677.

HOGG R., HEALY T. W., and FUERSTENAU D. W. (1966) Mutual coagulation of colloidal dispersions. *Trans. Faraday Soc.* **62,** 1638–1651.

HORZEMPA L. M. and HELZ G. R. (1979) Controls on the stability of sulfide sols: Colloidal covellite as an example. *Geochim. Cosmochim. Acta* **43,** 1645–1650.

HOUGH D. B. and WHITE L. R. (1980) The calculation of Hamaker constants from Lifshitz theory with applications to wetting phenomena. *Adv. Colloid Interface Sci.* **14,** 3–41.

JAMES R. O. and HEALY T. W. (1972) Adsorption of hydrolyzable metal ions at the oxide-water interface II. Charge reversal of SiO_2 and TiO_2 colloids by adsorbed Co(II), La(III), and Th(IV) as model systems. *J. Colloid Interface Sci.* **40,** 53–64.

KÄMPF N. and SCHWERTMANN U. (1982) Goethite and hematite in a climosequence in southern Brazil and their application in classification of kaolinitic soils. *Geoderma* **29,** 27–39.

KHILAR K. C. and FOGLER H. S. (1984) The existence of a critical salt concentration for particle release. *J. Colloid Interface Sci.* **101,** 214–224.

KIA S. F., FOGLER H. S., and REED M. G. (1987) Effect of pH on colloidally induced fines migration. *J. Colloid Interface Sci.* **118,** 158–168.

KIMMEL G. E. and BRAIDS O. C. (1980) Leachate plumes in ground water from Babylon and Islip landfills, Long Island, New York. USGS Prof. Paper 1085.

LANGMUIR D. (1969) Geochemistry of iron in a coastal-plain groundwater of the Camden, New Jersey area. USGS Prof. Paper 650-C, C224–C235.

LANGMUIR D. (1971) Particle size effect on the reaction goethite = hematite + water. *Amer. J. Sci.* **271,** 147–156.

LIM C. H. and JACKSON M. L. (1982) Dissolution for total analysis. In *Methods of Soil Analysis, Part 2* (ed. A. L. PAGE) pp. 5–7. Amer. Soc. Agro.

LITTLE S. (1979) Fire and plant succession in the New Jersey Pine Barrens. In *Pine Barrens: Ecosystem and Landscape* (ed. R. T. T. FORMAN) pp. 297–314. Academic Press.

LORD D. G., BARRINGER J. L., JOHNSSON P. A., SCHUSTER P. F., WALKER R. L., FAIRCHILD J. E., SROKA B. N., and JACOBSEN E. (1990) Hydrogeochemical data from an acidic deposition study at McDonalds Branch basin in the New Jersey Pinelands, 1983–1986. USGS Open-File Rp. 88-500.

MAGARITZ M., AMIEL A. J., RONEN D., and WELLS M. C. (1990) Distribution of metals in a polluted aquifer: A comparison of aquifer suspended material to fine sediments of the adjacent environment. *J. Contam. Hydrol.* **5,** 333–347.

MARKEWITZ F. J. (1969) Ilmenite deposits of the New Jersey Coastal Plain. In *Geology of Selected Areas in New Jersey and Eastern Pennsylvania and Guidebook of Excursions* (ed. S. SUBITZKY) pp. 363–382. Rutgers Univ. Press.

MATLACK K. S., HOUSEKNECHT D. W., and APPLIN K. R. (1989) Emplacement of clay into sand by infiltration. *J. Sediment. Petrol.* **59,** 77–87.

MINARD J. R. (1966) Sandblasted blocks on a hill of the Coastal Plain of New Jersey. USGS Prof. Paper 550-B, B87–B90.

MOLENAAR N. (1986) The interrelation between clay infiltration, quartz cementation, and compaction in Lower Givetian terrestrial sandstones, northern Ardennes, Belgium. *J. Sediment. Petrol.* **56,** 359–369.

MORAD S. and ALDAHAN A. A. (1986) Alteration of detrital Fe-Ti oxides in sedimentary rocks. *Bull. GSA* **97,** 567–578.

MORAES M. A. S. and DE ROS L. F. (1990) Infiltrated clays in fluvial Jurassic sandstones of Reconcavo Basin, northeastern Brazil. *J. Sediment. Petrol.* **60,** 809–819.

NICHOLSON R. V., CHERRY J. A., and REARDON E. J. (1983) Migration of contaminants in groundwater at a landfill: A case study. 6. Hydrogeochemistry. *J. Hydrol.* **63,** 131–176.

OLSSON R. K. (1963) Latest Cretaceous and earliest Tertiary stratigraphy of New Jersey Coastal Plain. *Bull. AAPG* **47,** 643–665.

OWENS J. P., HESS M. M., DENNY C. S., and DWORNIK E. J. (1983) Postdepositional alteration of surface and near-surface minerals in selected Coastal Plain formations of the Middle Atlantic states. USGS Prof. Paper 1067-F, F1–F45.

PARKS G. A. (1967) Aqueous surface chemistry of oxides and complex oxide minerals. In *Equilibrium Concepts in Natural Water Systems* (ed. W. STUMM); Adv. Chem. Ser. 67, pp. 121–160. ACS.

PASSARETTI M. L. and ESLINGER E. V. (1987) Dissolution and relic textures in framework grains of Holocene sediments from the Brazos River and Gulf Coast of Texas. *J. Sediment. Petrol.* **57,** 94–97.

PENROSE W. R., POLZER W. L., ESSINGTON E. H., NELSON D. M., and ORLANDINI K. A. (1990) Mobility of plutonium and americium through a shallow aquifer in a semiarid region. *Environ. Sci. Tech.* **24,** 228–234.

POPPE L. J. and HATHAWAY J. C. (1979) A metal-membrane mount for X-ray powder diffraction. *Clays Clay Mineral.* **27,** 152–153.

POSTMA D. and BROCKENHUUS-SCHACK B. S. (1987) Diagenesis of iron in proglacial sand deposits of late- and post-Weichselian age. *J. Sediment. Petrol.* **57,** 1040–1053.

RHODEHAMEL E. C. (1979a) Geology of the Pine Barrens of New Jersey. In *Pine Barrens: Ecosystem and Landscape* (ed. R. T. T. FORMAN) pp. 39–60. Academic Press.

RHODEHAMEL E. C. (1979b) Hydrology of the New Jersey Pine Barrens. In *Pine Barrens: Ecosystem and Landscape* (ed. R. T. T. FORMAN) pp. 39–60. Academic Press.

RUCKENSTEIN E. and PRIEVE D. C. (1976) Adsorption and desorption of particles and their chromatographic separation. *Amer. Inst. Chem. Eng. J.* **22,** 276–283.

RYAN J. N. and GSCHWEND P. M. (1990) Colloid mobilization in two Atlantic Coastal Plain aquifers: Field studies. *Water Resources Res.* **26,** 307–322.

RYAN J. N. and GSCHWEND P. M. (1991) Extraction of iron oxides from sediments using reductive dissolution by titanium(III). *Clays Clay Mineral.* **39,** 509–518.

SCHINDLER P. W., FÜRST B., DICK R., and WOLF P. U. (1976) Ligand properties of surface silanol groups I. Surface complex formation with Fe^{3+}, Cu^{2+}, Cd^{2+}, and Pb^{2+}. *J. Colloid Interface Sci.* **55,** 469–475.

SCHLUGER P. R. and ROBERSON H. E. (1975) Mineralogy and chemistry of the Patapsco Formation, Maryland, related to the groundwater geochemistry and flow system: A contribution to the origin of red beds. *Bull. GSA* **86,** 153–158.

SCHULZE D. G. (1984) The influence of aluminum of iron oxides. VIII. Unit-cell dimensions of Al-substituted goethites and estimation of Al from them. *Clays Clay Minerol.* **32,** 36–44.

SCHWERTMANN U. (1988) Occurrence and formation of iron oxides in various pedoenvironments. In *Iron in Soils and Clay Minerals* (ed. J. W. STUCKI, B. A. GOODMAN, and U. SCHWERTMANN) pp. 267–308. D. Reidel.

SHORT S. A., LOWSON R. T., and ELLIS J. (1988) $^{234}U/^{238}U$ and $^{230}Th/^{234}U$ activity ratios in the colloidal phases of aquifers in lateritic weathered zones. *Geochim. Cosmochim. Acta* **52,** 2555–2563.

TARDY Y. and NAHON D. (1985) Geochemistry of laterites, stability of Al-goethite, Al-hematite, and Fe^{3+}-kaolinite in bauxites and ferricretes: An approach to the mechanism of concretion formation. *Amer. J. Sci.* **285,** 865–903.

TAYLOR R. M., RAUPACH M., and CHARTRES C. J. (1990) Simulation of soil reactions: Aluminum-iron (III) hydroxy species react with silica to give deposits on particle surfaces. *Clay Minerals* **25,** 375–389.

TEMPLE A. K. (1966) Alteration of ilmenite. *Econ. Geol.* **61,** 695–714.

TEUFER G. and TEMPLE A. K. (1966) Pseudorutile—A new mineral intermediate between ilmenite and rutile in the N alteration of ilmenite. *Nature* **211,** 179–181.

TURNER-PETERSON C. E. (1985) Lacustrine-humate model for primary uranium ore deposits, Grants Uranium Region, New Mexico. *Bull. AAPG* **69,** 1999–2020.

VERWEY E. J. W. and OVERBEEK J.Th.G. (1948) *Theory of the Stability of Lyophobic Colloids.* Elsevier.

WALKER T. R. (1967) Formation of red beds in modern and ancient deserts. *GSA Bull.* **78,** 353–368.

WALKER T. R. (1974) Formation of red beds in moist tropical climates: A hypothesis. *Bull. GSA* **85,** 633–638.

WALKER T. R. (1976) Diagenetic origin of continental red beds. In *The Continental Permian in Central, West, and South Europe* (ed. H. FALKE) pp. 240–482. D. Reidel.

WALKER T. R., WAUGH B., and CRONE A. J. (1978) Diagenesis in first-cycle desert alluvium of Cenozoic age, southwestern United States and northwestern Mexico. *Bull. GSA* **89,** 19–32.

WESTALL J. C., ZACHARY J. L., and MOREL F. M. M. (1976) MINEQL: A computer program for the calculation of chemical equilibrium composition of aqueous systems. Tech. Note 18, R. M. Parsons Lab, Dept. Civil Eng., MIT.

YAO K.-M., HABIBIAN M. T., and O'MELIA C. R. (1971) Water and wastewater filtration: Concepts and applications. *Environ. Sci. Tech.* **11,** 1105–1112.